Noname manuscript No.
(will be inserted by the editor)

A Plug-and-Play Coupling Approach for Parallel Multi-Field Simulations

Hans-Joachim Bungartz, Florian Lindner, Miriam Mehl, Benjamin Uekermann

Received: date / Accepted: date

Abstract For multi-field simulations involving a larger number of different physical fields and in cases where the involved fields or simulation codes change due to new modelling insigts, e.g., flexible and robust partitioned coupling schemes are an important prerequisite to keep time-to-solution within reasonable limits. They allow for a fast, almost plug-and-play combination of existing established codes to the respective multi-field simulation environment. In this paper, we study a class of coupling approaches that we originally introduced in order to improve the parallel scalability of partitioned simulations. Due to the symmetric structure of these coupling methods and the use of 'long' vectors of coupling data comprising the input and output of all involved codes at a time, they turn out to be particularly suited also for simulations involving more than two coupled fields. As standard two-field coupling schemes are not suited for such cases as shown in our numerical results, this allows the simulation of a new range of applications in a partitioned way.

Keywords multi-field simulation · strong coupling · partitioned approach

Hans-Joachim Bungartz, Benjamin Uekermann
Department of Computer Science
Technische Universität München
Boltzmannstraße 3
85748 Garching, Germany
{bungartz,uekerman}@in.tum.de

Florian Lindner, Miriam Mehl
Institute for Parallel and Distributed Systems, Universität Stuttgart
Universitätsstraße 38
70569 Stuttgart, Germany
{florian.lindner,miriam.mehl}@ipvs.uni-stuttgart.de

1 Introduction

The simulation of the interaction between three or more physical fields, so-called multi-physics scenarios, is crucial in many engineering or biomedical applications. This includes, for example, fluid-structure-acoustic interaction (e.g. [12]), where the acoustic field can be seperated in a complex near field and a simplified far field, or simulations of the heart, where electro-magnetism, fluid flow, and structure equations are coupled ([11]). Also scenarios with multiple flow fields such as partially filled tanks on container ships ([7]) belong to this class. If the coupling is restricted to a lower-dimensional manifold in the computational domain, which is the case in the mentioned examples, we speak of surface-coupled problems. Two-physics versions of such applications, in particular fluid-structure interactions, have been widely simulated with partitioned approaches until more and more monolithic methods and codes have evolved throughout the last years. In purely monlithic approaches, a completely new software for a specific set of coupled equations is developed that solves the large coupled system as a whole. Although monolithic approaches are very efficient to tackle established multi-physics applications where neither the fields nor the used discretization methods are expected to change drastically over a long time period, they imply an unfeasible complexity, if a varying set of physical fields and discretization methods is considered. Direct coupling and quasi-direct coupling methods were developed for fluid-structure simulations in [1] that deliberately use nonmatching meshes at the fluid-structure interface and reduce to monolithic methods for matching grids. These methods, to some degree, make the overall FSI solver environment more modular. The connection at non-matching grid interfaces is established

via suitable projection equations, which are solved using sublevel iterations. However, often black-box solvers that allow to access only input-output information are to be used. Here, the partitioned approach comes into play that splits the physical domain into single-physics fields, simulates all fields with their own solvers, and couples these solvers via common interfaces. This gives us the possibility to reuse existing software and, thus, considerably speed up the code development time. As long as the coupling is restricted to a surface (instead of the whole volume of the domain), the amount of data to be transferred between the solvers is comparable to the amount of data transferred in a distributed memory parallelization of the single fields which makes the partitioning feasible in terms of runtime performance.

However, the splitting into single fields possibly introduces stability issues that need to be tackled by advanced coupling algorithms. Depending on the type of interaction between the single physical fields, the task of finding a stable and accurate coupling method can be easy or rather difficult. We speak of a uni-directional interaction if the mutual influence between two physical fields P_i and P_j is only one-sided, e.g., P_i influences P_j but not vice versa. Such problems can be handled easily and efficiently even with a file-based one-time data transfer between the single field solvers and is, therefore, not considered in this paper. We focus on bi-directional interactions where both fields have an impact on each other. Depending on the strength of the bi-directional interaction, more or less sophisticated methods are required for the numerical coupling of the fields.

For coupling of only two fields which we refer to as bi-coupling schemes in the following, a variety of partitioned methods from explicit schemes (executing only a fixed number of single field solves per multi-field time step [5]) to stable implicit schemes (iterating between the single field solvers until the time step equation converges to the monolithic solution) are known from literature. Explicit coupling schemes are known to yield stable time-stepping only in cases with a relatively weak bi-directional coupling. Implicit schemes are particularly necessary for fluid-structure interaction (FSI) with incompressible fluids, a typical case for a strong bi-directional interaction due to the so-called added mass effect (e.g. [3,2]). Established stable iteration methods are Aitken underrelaxation ([10]), or quasi-Newton methods ([4,19,14,15])[1]. Usually, these methods execute the single field solvers in a staggered way, i.e., one after the other which limits the scalability of such a simulation on massively parallel systems. As massively parallel computations are necessary for multi-physics scenarios, since only a high resolution of all fields allows to take advantage of the more complex modeling of multi-physics scenarios compared to single-physics scenarios, we developed implicit coupling algorithms executing the involved single field solvers in parallel to each other ([17,13]).

Whereas many coupling algorithms for systems involving two surface-coupled physical fields have been developed in the last decade, there are hardly any general and robust methods available for the coupling of multiple fields. In [16], a multi-coupling algorithm that needs full Jacobian information (non-black-box) is described and tested for lower dimensional problems. The necessity of full Jacobian information makes it very cumbersome to integrate this algorithm in 2D or 3D scenarios already in the case of non-black-box solvers.

In this work, we develop and discuss multi-coupling algorithms that are derived from either a simple composition of bi-coupling schemes or a generalization of the underlying idea of our parallel coupling to a true multi-coupling. To our knowledge, this is the first time, that a fully-implicit black-box multi-coupling algorithm is described that allows to simulate scenarios in a partitioned way. The results in Sects. 6 and 8 show that the easiest approach, i.e., the composition of bi-coupling schemes, is not sufficient already for moderately difficult problems.

The remainder of this work is organized as follows: A model problem containing three different physical fields is introduced in 2. Section 3 shortly recalls the staggered and our parallel bi-coupling approach based on IQN coupling schemes. Based on this, we propose different multi-field coupling methods for the example of the model problem from Sect. 2 in Sect. 4. Section 5 shortly introduces the inhouse coupling software preCICE in which all coupling methods are implemented. A first set of numerical results for our model problem is presented in Sect. 6. Sect. 7 generalizes the ideas of our multi-coupling approach to general multi-field scenarios, followed by a second set of numerical results for a further academic multi-coupling scenarion in Sect. 8. Finally, Sect. 9 concludes this work with some preliminary guidelines how to choose the optimal multi-coupling scheme for a particular scenario.

2 A Fluid-Structure-Fluid Model Problem

For the sake of clarity, we start with a model problem comprising three solvers, two fluid solvers F_1 and

[1] In block-iterative coupling and partitioned approaches with direct access to discretization details, increasing the entries of the structural mass matrix is a further possible stabilization technique that dates back to 2003 and earlier (see [1] and citations therein)

F_2 and one structural solver S solving a scenario with two (possibly different) fluids separated by an elastic structure. As the two fluid solvers do not have a direct interaction with each other, this model scenario corresponds to the graph shown in Figure 1.

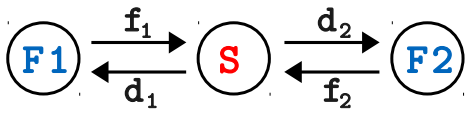

Fig. 1 Multi-physics model problem, represented in a dependency graph. Two fluid solvers F_1 and F_2 compute force values f_1 and f_2, acting as input values for the structural solver S, who itself gives back displacement values d_1 and d_2 to the fluid solvers.

This model problem contains already many basic issues of general multi-physics scenarios. Therefore, we use it to study various multi-coupling approaches without the formalism needed to describe general multi-physics problems. We want to stress that all techniques developed in this work can be generalized in a straightforward way to problems comprising more than three physical solvers as sketched in Section 7. Also the implementation in `preCICE` allows for more complicated scenarios.

The densities ρ_{F1}, ρ_{F2}, and ρ_S in all three physical domains and the geometrical shape of the structural domain determine the strength of the three-field interaction, and, thus, have a crucial impact on the suitability and performance of coupling schemes. We use this fact to study different setups with strong or weak interaction between all three fields as well as strong interaction between two fields and weak interaction with the third field in Section 6. We introduce a variety of coupling approaches and discuss their theoretical applicability in the following two sections.

3 A Short Review of Staggered and Parallel Two-Field Coupling

As our multi-field coupling ideas are based on our developments for parallel two-field coupling, we shortly recall the underlying ideas in this section. The basis of our parallel coupling approach is the following observation: Each multi-physics problem can be reformulated as a fixed-point equation (FPE). This is widely used in classical partitioned FSI problems, where many coupling algorithms are derived from the FPE

$$(S \circ F)(d) = d \, . \tag{1}$$

where S and F denote the structure and the flow solver, respectively, d is the displacement (or the velocity) of the structure surface. Below, f is the force exerted on the structure surface by the fluid. We showed in [17,13], that the same solution is achieved from the alternative FPE in matrix-like notation

$$\begin{pmatrix} 0 & F \\ S & 0 \end{pmatrix} \begin{pmatrix} f \\ d \end{pmatrix} = \begin{pmatrix} f \\ d \end{pmatrix} \, , \tag{2}$$

which we refer to as the vectorial system. The two fixed-point equations are associated to two different execution orders of flow and structure solver in an iterative solution method as shown in Fig. 2. Thus, the second fixed-point equation has the advantage that the fluid and the structure solver can be executed in parallel to each other leading to a better parallel efficiency. In Sect. 4.2, we use a similar idea to get from combinations of bi-coupling methods to a true multi-field coupling.

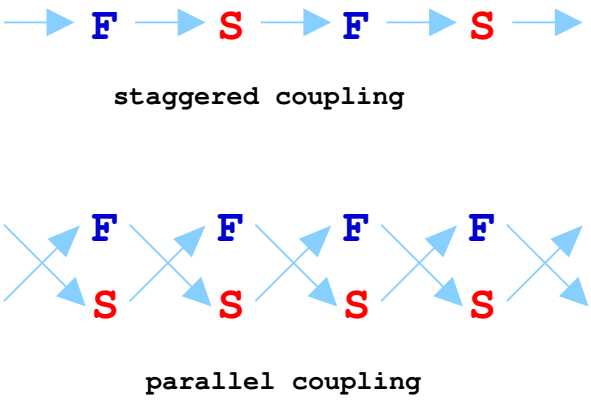

Fig. 2 Schematic view of the execution order of fluid and structure solvers for the standard staggered approach corresponding to the staggered fixed-point equation (1) and the parallel coupling approach corresponding to the parallel fixed-point equation (2).

Before proceeding to multi-field coupling, we should, however add some remarks on suitable solution methods for the parallel fixed-point equation (2). We showed in [13] that simple FPE solvers such as a fixed-point iteration or an Aitken underrelexation for classical FSI problems lead to a two times slower convergence when using (2) compared to (1). Sophisticated quasi-Newton FPE solvers, based on the solution of a least-squares system in every iteration, however, show only a slight degradation of the convergence rate. Such a quasi-Newton least-squares (QNLS) solver (cf. [8]) was applied for (1) in [4] based on similar ideas in [14,19] and for (2) in [17,13]. Algorithm 1 describes the QNLS technique for a general fixed-point equation $H(x) = x$. In a transient setting, the reuse of iteration values from previous time steps can lead to a far better efficiency (cf. [4,13]).

We write QNLS(n) for a quasi-Newton solver reusing information from n time steps.

Algorithm 1 Quasi-Newton least squares method in pseudocode (cf. [4,8])

initial value x^0
$\tilde{x}^0 = H(x^0)$ and $R^0 = \tilde{x}^0 - x^0$
$x^1 = x^0 + 0.1 \cdot R^0$
for $k = 1 \ldots$ **do**
  $\tilde{x}^k = H(x^k)$ and $R^k = \tilde{x}^k - x^k$
  if $\|R^k\|/\|x^k\| < \epsilon$: **break**
  $V^k = [\Delta R_0^k, \ldots, \Delta R_{k-1}^k]$ with $\Delta R_i^k = R^i - R^k$
  $W_k = [\Delta \tilde{x}_0^k, \ldots, \Delta \tilde{x}_{k-1}^k]$ with $\Delta \tilde{x}_i^k = \tilde{x}^i - \tilde{x}^k$
  decompose $V^k = Q^k U^k$
  solve the first k lines of $U^k \alpha = -{Q^k}^T R^k$
  $\Delta \tilde{x} = W\alpha$
  $x^{k+1} = \tilde{x}^k + \Delta \tilde{x}^k$
end for

4 Options for Multi-Field Coupling

4.1 Composition of Bi-Coupling Schemes

This section discusses methods for multi-coupling that can be easily derived (and implemented) as a combination of existing bi-coupling methods. There are basically two ways to combine bi-couplings: concatenation (Section 4.1.1) and inclusion (Section 4.1.2).

4.1.1 Concatenation of Bi-Coupling Schemes

The straightforward idea to couple multiple physical solvers P_i is to use a bi-coupling scheme for each edge in the multi-physics graph as displayed in Figure 3 for our model problem from Section 2. In this setting, each bi-coupling scheme can be adjusted to meet particular needs. In particular, we can choose whether an explicit or an implicit scheme is required for each bi-coupling separately. Figure 4 shows that different choices lead to different execution orders of the physical solvers. All combinations sketched in Figure 4 are supported in `preCICE` (cf. [6] and Section 5). If two implicit schemes are used, they do, in general, not convergence at the same time. In this case, the early converged coupling scheme waits until convergence of all schemes.

Sophisticated implicit coupling schemes such as Aitken underrelaxation or quasi-Newton methods reuse information collected over several iterations to estimate the response of the coupled system and, finally, to choose the best coupling parameters. If we concatenate bi-coupling schemes, we introduce an artificial decomposition into pairs of coupled solvers. I.e., we apply fixed-point solvers to smaller systems that each contains only two fields. Combining two IQN solvers for our model problem in the way sketched in the lower left graph in Fig. 4, this means that we aim at solving

$$\begin{pmatrix} d1 \\ d2 \end{pmatrix} = S \circ \begin{pmatrix} F1 & 0 \\ 0 & F2 \end{pmatrix} \begin{pmatrix} d1 \\ d2 \end{pmatrix}$$

by decomposing it into the two equations

$d1 = S_{f2} \circ F1(d1)$ and

$d2 = S_{f1} \circ F2(d2)$.

Note that the subscripts $\cdot_{f1}$ and $\cdot_{f2}$ indicate that the response of the structure solver applied to the result of one of the two fluid solvers at the same time depends on the result of the other fluid solver. This implies that, if both coupling schemes are implicit, they hamper each other since the response of the two corresponding fixed-point operators $S_{f2} \circ F1$ and $S_{f1} \circ F2$ changes with $f1$ and $f2$. Similar considerations apply for the case of a concatenation of two instances of our parallel implicit coupling schemes introduced in [17,13]. This type of concatenation is shown in the lower right picture in Fig. 4 where we solve the two subsystems

$$\begin{pmatrix} 0 & F1 \\ S_{f2} & 0 \end{pmatrix} \begin{pmatrix} f1 \\ d1 \end{pmatrix} = \begin{pmatrix} f1 \\ d1 \end{pmatrix} \quad \text{and}$$

$$\begin{pmatrix} 0 & F2 \\ S_{f1} & 0 \end{pmatrix} \begin{pmatrix} f2 \\ d2 \end{pmatrix} = \begin{pmatrix} f2 \\ d2 \end{pmatrix}.$$

In mathematical terms, this means that the Jacobian of both two-field subsystems in the three-field system changes substantially throughout the iterations. This makes it almost impossible for the third solver to get any useful information on the response of such a subsystem. This is especially a problem if both fluid solvers F_1 and F_2 are indirectly strongly coupled which is the case for a very thin, elastic or lightweight structure. The impact of the described problem, depends, thus, on the geometrical shape and the stiffness of S. Numerical experiments in Sect. 6 confirm this conclusion. Obviously, this problem reappears in general multi-physics problems, if multiple implicit bi-coupling schemes influence each other. A simple concatenation of bi-coupling schemes does, in general, not result in a stable overall coupling. In Sections 4.1.2 and 4.2, we present possible remedies.

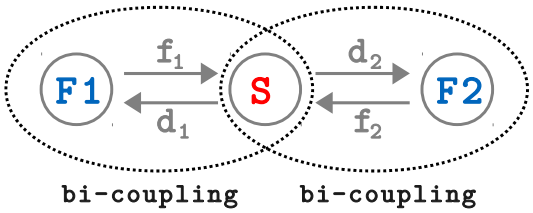

Fig. 3 Schematic view of the three-field coupling for the model problem from Section 2 using a concatenation of two bi-coupling methods, one for each edge in the interaction graph.

4.1.2 Inclusion of Bi-Coupling Schemes

The alternative to a simple concatenation of bi-coupling schemes is the inclusion of bi-coupling schemes. Here, two physical solvers coupled by a bi-coupling scheme are regarded as an entity from the outside and are coupled with the third solver using a bi-coupling approach again. Figure 5 shows a variant of this approach for our model problem: F_1 and S are bi-coupled and the converged entity (F_1S) is bi-coupled with F_2. Different from the methods in Section 4.1.1, this implies, that we have induced a nesting of iterations: In the inner iteration, we iterate between F_1 and S until convergence to the two-field monolithic solution. The result is then transferred to F_2 which returns its result to S. This outer coupling is then repeated until convergence to the three-field system. If we assume that M iterations are required for both the inner and the outer iteration, a total of M^2 solves is required for F_1 and S, whereas M solves are needed for F_2. Only if we apply an explicit scheme to the outside coupling, the overall scheme does not differ from a concatenation scheme.

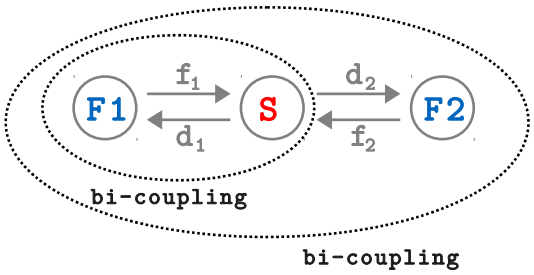

Fig. 5 Schematic view of the three-field coupling for the model problem from Section 2 using an inclusion of two bi-coupling methods. Two coupled physical solvers are regarded as an entity from the outside and are coupled with the third solver. If two implicit schemes are applied, this results in two nested iteration loops.

We suppose that the inclusion of two implicit schemes always results in an overall stable coupling if we choose appropriate methods for each of the bi-couplings. The disadvantage of a multiple inclusion is its computational cost: the number of solver executions grows exponentially with the number of physical fields if we assume that each coupling schemes needs a constant amount of iterations. This is the reason, why we did not implement such schemes in `preCICE`. In the next section, we develop a far more efficient and stable multi-coupling scheme.

4.2 Multi-Coupling Schemes

In this section, we generalize our parallel bi-coupling schemes to proper multi-coupling schemes by directly looking at the coupling of multiple solvers as depicted in Figure 6.

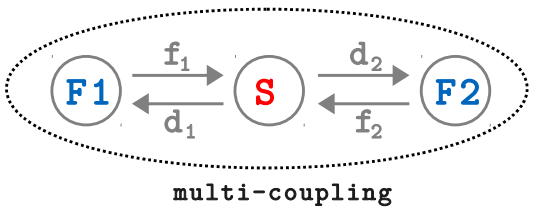

Fig. 6 Schematic view of the three-field coupling for the model problem from Section 2 using a multi-coupling approach, i.e. considering all interactions in an overall coupling system.

We've already used different types of fixed-point equations in Sects. 4.1.1 and 3 who's solution leads to the monolithic solution of the respective coupled multi-field problem. For our three-field model problem, we could also execute all three involved solvers in parallel to each other. If we (as in the step from staggered to parallel flud-structure coupling) leave the in- and output relations of all three solver unchanged, this corresponds to the iteration

$$\begin{pmatrix} f_1^{it+1} \\ f_2^{it+1} \\ \begin{pmatrix} d_1^{it+1} \\ d_2^{it+1} \end{pmatrix} \end{pmatrix} = \begin{pmatrix} F1(d_1^{it}) \\ F2(d_2^{it}) \\ \\ S(f_1^{it}, f_2^{it}) \end{pmatrix}$$

if we don't use any underrelaxation or quasi-Newton convergence acceleration. Thus, written in matrix-like form, we solve the fixed-point equation

$$\begin{pmatrix} 0 & 0 & F1 & 0 \\ 0 & 0 & 0 & F2 \\ S_{11} & S_{12} & 0 & 0 \\ S_{21} & S_{22} & 0 & 0 \end{pmatrix} \begin{pmatrix} f_1 \\ f_2 \\ d_1 \\ d_2 \end{pmatrix} = \begin{pmatrix} f_1 \\ f_2 \\ d_1 \\ d_2 \end{pmatrix}. \tag{3}$$

This FPE can now be solved with any FPE solver. Again, the quasi-Newton method mentioned above in Sect. 3 is a very powerful solver. If a quasi-Newton least squares method reusing the information of n previous time steps is applied for a complete multi-physics problem such as (3), we refer to the coupling scheme as the "multi interface quasi-Newton" scheme (MIQN(n)).

The fixed-point x that Algorithm 1 seeks for consists, in our model problem, of the four different subvectors f_1, f_2, d_1, and d_2. The solution of the least-squares system in QNLS (Algorithm 1 uses a QR-decomposition),

depends highly on the mutual scaling of those subvectors. In classical FSI applications, force vectors often have substantially larger values than the displacements, in particular if displacement increments are used instead of absolute displacements relative to the initial state. In order to balance the influence of all subvectors we, thus, have to apply a normalization. In our studies, we found that a static scaling of the force vectors results in a sufficiently good balance. The potential of further improvements if using a dynamical scaling is subject of further research.

5 The Coupling Software preCICE

All coupling methods used in Section 6 are implemented in `preCICE`, a coupling library ([6]) developed in our group, which offers, besides different coupling algorithms, also methods for mapping data between non-matching meshes and communication routines. The application interface of `preCICE` is formulated on a very high level, allowing for a minimally invasive inclusion in any single-physics code. Once a solver is adapted to `preCICE`, different other solvers can be coupled in a nearly plug-and-play manner. Different solvers including commercial tools such as `Fluent` or `COMSOL`, open source tools such as `OpenFOAM`, and in-house codes (e.g. [18]), have been coupled successfully to `preCICE`. `preCICE` itself is open-source software[2]. For sake of brevity, implementation details of `preCICE` are left out in this work. The interested reader is referred to [6].

6 Numerical Results: Fluid-Structure-Fluid

6.1 Experiment Settings

Figure 7 depicts the geometry of the scenario that we study numerically. Two fluid domains F_1 and F_2 are separated by an elastic beam S, which is fixed on both ends. We distinguish two variants, which differ in the vertical extent of the beam: one thin variant S_1, $d_1 = 0.2$, and one thick variant S_2, $d_2 = 1.0$. The thin variant induces a stronger indirect interaction between the two fluid fields than the thick variant. The structure is modeled by a St. Venant-Kirchoff cantilever with Young's modulus $E = 5.6 \cdot 10^6$ kg/ms^2 and Poisson-ratio 0.4 . The density of the structure varies from 10^2 to 10^3 kg/m^3. Both fluids are modeled by the incompressible Navier-Stokes equations, with dynamic viscosity $\mu = 10^2$ kg/ms. The inflows show a parabolic velocity profile with mean velocity $U = 1.0$ m/s. The

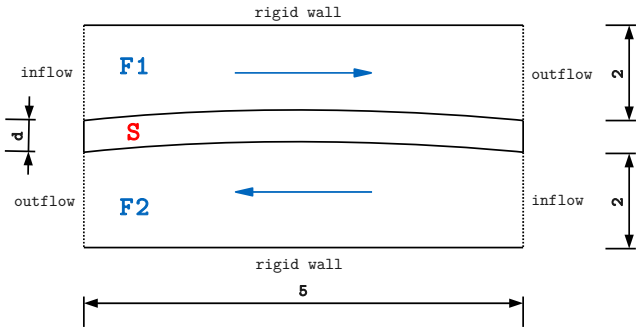

Fig. 7 Scenario sketch: 2 fluid domains F_1 and F_2 are separated by an elastic beam S, which is fixed on both ends. Two variants of this scenario are studied, which differ in the vertical extent of the beam, $d_1 = 0.2$ or $d_2 = 1$ m.

densities of both fluids, ρ_{F1} and ρ_{F2}, vary separately in the range from 10^0 to 10^3 kg/m^3, leading to either weak or strong interactions between both fluids and the structure.

We use `Alya`[3] as the physical solver for all three domains (cf. [18,9]). There is, however, no particular need for this choice. Solvers can be exchanged in a nearly plug-and-play manner to meet particular needs. We showed, for example, in [13] the bi-coupling of `COMSOL`, `Fluent`, or `OpenFOAM`. Both fluid domains are discretized with approximately 4000 elements each, whereas the structure consists of approximately 2250 (S_1), respectively 600 (S_2) elements. We use a matching grid at both interfaces. `Alya` uses finite elements for both, structure und fluids. The moving structure is resolved in the fluid by an arbitrary Lagrangian-Eulerian perspective, involving the movement of the underlying grid. For further numerical details of `Alya`, we want to refer to [18]. The timestep size is set to $dt = 10^{-3}$ s. To decide on the overall convergence, we use relative convergence criteria of 10^{-3} for all coupling variables, displacement increments and forces on both interfaces. Figure 8 shows the results for the thin structure at $t = 1.0$ s

6.2 Discussion

This subsection presents and discusses the results for the test case described above. We vary the density of all three physical fields and the thickness of the structure. From literature (e.g. [3,2]), we know that the interaction between fluid and structure gets stronger, and thus the coupling gets more elaborate, if the density ratio

[2] `http://www5.in.tum.de/wiki/index.php/PreCICE_Webpage`

[3] `Alya` is developed at the Barcelona Supercomputing Center, cf. `http://www.bsc.es/computer-applications/alya-system`.

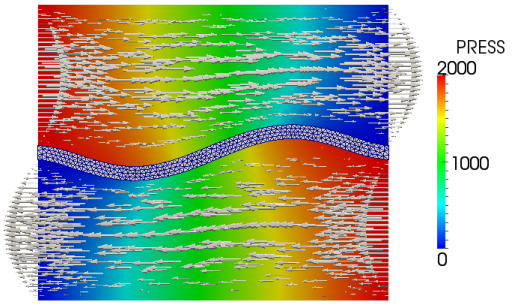

Fig. 8 Pressure values (N/m^2), velocity vectors and grid deformation for the fluid-structure-fluid model problem at $t = 1.0$. This run uses the thin structure S_1, the densities $\rho_{F1} = \rho_{F2} = 10^3$ kg/m^3, $\rho_S = 10^1$ kg/m^3, and the MIQN(8) coupling scheme. For sake of clarity, the structural displacements are scaled by a factor of 5.

ρ_{F1} - ρ_S - ρ_{F2}	Coupling	S_1	S_2
10^0 - 10^3 - 10^3	CSS / IQN(5)	4.62	4.62
10^0 - 10^3 - 10^3	CSS / IQN(0)	9.04	9.24
10^1 - 10^3 - 10^3	CSS / IQN(5)	crash	crash
10^1 - 10^3 - 10^3	IQN(5) / IQN(5)	crash	3.08 / 4.56
10^2 - 10^3 - 10^3	IQN(5) / IQN(5)	crash	crash
10^3 - 10^3 - 10^3	IQN(5) / IQN(5)	crash	5.10 / 5.18
10^3 - 10^2 - 10^3	IQN(5) / IQN(5)	crash	crash
10^3 - 10^1 - 10^3	IQN(5) / IQN(5)	crash	crash
10^1 - 10^3 - 10^3	MIQN(8)	5.64	5.62
10^2 - 10^3 - 10^3	MIQN(8)	5.88	5.76
10^3 - 10^3 - 10^3	MIQN(8)	7.40	7.00
10^3 - 10^2 - 10^3	MIQN(8)	11.78	11.72
10^3 - 10^1 - 10^3	MIQN(8)	20.90	17.20

Table 1 Average iteration numbers needed for convergence for various coupling configurations and different density ratios (all values in kg/m^3). S_1 and S_2 refer to the thin respectively thick structure. The values are averaged over the first 50 timesteps. The upper part shows results for the concatenation of an explicit and an implicit scheme, the middle part for the concatenation of two implicit schemes (cf. Section 4.1.1), and the lower part for the newly developed multi-coupling scheme (cf. Section 4.2).

ρ_F/ρ_S raises. Furthermore, by lowering the thickness of the structure, we can raise the indirect interaction between both fluid fields. Table 1 shows the average iteration numbers per timestep, listed for various density ratios, for both structures, and for the different coupling schemes, we introduced in Sections 4.1 and 4.2. By "IQN(5) / IQN(5)", we denote a concatenation of two interface quasi-Newton schemes (developed in [4]), with re-used information from 5 timesteps, whereas CSS refers to the classical serial staggered scheme (the trivial explicit scheme, discussed in [5]). MIQN is the multi quasi-Newton coupling scheme, introduced in Section 4.2. Our experiences in [13] determined the choice of reused timesteps. For the MIQN scheme, we scale all force vectors by a factor of 10^{-7} (compare the discussion in Section 4.2).

In Table 1, we can observe several aspects. The upper part of the table shows results for a weak $F_1 - S$ interaction and a strong $F_2 - S$ interaction. For this case, we concatenate an explicit with an implicit scheme. We can argue from the results that, in this case, the strong interaction dominates the overall system. This means that the implicit coupling is not hampered by the explicit scheme. We can observe this in the better convergence of CSS / IQN(5) compared to CSS / IQN(0). If the density of F_1 is raised to 10^1 kg/m^3, the interaction between F_1 and S also becomes a strong one, leading to divergence if only an explicit scheme is used. In general, the behavior of the overall system, in this case, is very similar to the bi-coupling of F_2 and S itself. The thickness of the structure, in particular, has no important influence here.

The middle block of Table 1 shows results for two strong interactions, demanding an implicit scheme on both interfaces. The concatenation of two implicit schemes, however, is not successful, since both interface systems hamper each other (compare the explanation in Section 4.1.1). It is striking that this problem especially influences the test case with the thin structure S_1, since, here, both fluid fields possess a strong indirect interaction. In this case, all density settings lead to divergent runs. If the structure gets very thick, both interface systems get quasi independent from each other, and a concatenation of two implicit schemes can be successful. If we then lower the density of S, both interactions become stronger, and both interfaces influence each other again.

The lower block of Table 1 shows results for the same density settings, but now for the multi-coupling scheme MIQN. We observe a stable coupling for all settings. The number of iterations gets bigger for a stronger interaction between both fluid fields and the structure fields, but also for a stronger indirect interaction between both fluid fields.

7 Ways to Generalize the Coupling

Our multi-coupling schemes are easily extendable to arbitrary multi-field coupling. For a mathematical formulation, we have to introduce an abstract notation: To include also commercial tools with a closed application interface, i.e., black-box solvers, we describe the n single-field solvers G_i, $i = 1, 2, \ldots, n$ of an n-field coupled system simply by input-output relations

$$G_i : x_{i,\text{in}} \mapsto x_{i,\text{out}} \quad \text{for all} \quad i = 1, 2, \ldots, n.$$

Here, $x_{\text{in}} \in \mathbb{R}^N$ denotes a vector of nodal input values at the discretized coupling surface between G_i and other physical fields. P_i maps this input to output values $x_{\text{out}} \in \mathbb{R}^N$ by calculating one timestep or one iteration. A fluid solver in a so-called Dirichlet-Neumann coupling, for example, gets displacement values from (possible multiple) structure solvers at a common surface, calculates new pressure and velocity values, and finally gives back force values to the structure solvers at the same coupling surface.

In general, we can model surface-coupled multi-physics scenarios as directed graphs where each vertex corresponds to a physical solver P_i and each edge from solver P_i to G_j means that the output (or part of it) of P_i is an input variable of G_j. Note that this can either be in terms of actual physical coupling or in terms of the modelling of the coupling. In our model, we might decide to approximate a bi-directional coupling by a uni-directional coupling or to even completely neglect some of the coupling relations. A possible representation of the coupling graph is an adjacency matrix A that has an entry $a_{ji} = 1$ if and only if the directed edge from G_i to G_j exists. All other entries are zero.

The full vectorial fixed-point problem involving all n single-field solvers $G_1, G_2, \ldots, G_n$ of our multi-field problem in parallel reads

$$P \begin{pmatrix} G_1 & 0 & \cdots & 0 \\ 0 & G_2 & \ddots & \vdots \\ \vdots & \ddots & \ddots & 0 \\ 0 & \cdots & 0 & G_n \end{pmatrix} \begin{pmatrix} x_{1,\text{in}} \\ x_{2,\text{in}} \\ \vdots \\ x_{n,\text{in}} \end{pmatrix} = \begin{pmatrix} x_{1,\text{in}} \\ x_{2,\text{in}} \\ \vdots \\ x_{n,\text{in}} \end{pmatrix}$$

where P is a permutation that reorders the output vectors of the solvers such that the composed vector can be used as an input for the next iteration. For our three-field model problem from Sect. 2, we, e.g., can rewrite the multi-coupling fixed point equation (3) as

$$\begin{pmatrix} 0 & I & 0 \\ 0 & 0 & I \\ \begin{pmatrix} I & 0 \\ 0 & I \end{pmatrix} & & 0 \end{pmatrix} \begin{pmatrix} F_1 & 0 & 0 \\ 0 & F_2 & 0 \\ 0 & 0 & S \end{pmatrix} \begin{pmatrix} d_1 \\ d_2 \\ \begin{pmatrix} f_1 \\ f_2 \end{pmatrix} \end{pmatrix} = \begin{pmatrix} d_1 \\ d_2 \\ \begin{pmatrix} f_1 \\ f_2 \end{pmatrix} \end{pmatrix}.$$

Before applying a multi-coupling for our whole multi-field system, we should in a first step identify decoupled subsystems (if any) and uni-directional coupling. As a formal tool, we can use the permutation matrix P. We can rewrite P in a block-wise manner using blocks $P_{i,j}$ defining which part of the output of solver G_j goes to which part of the input vector of solver G_i:

$$P = \begin{pmatrix} P_{1,1} & \cdots & P_{1,n} \\ \vdots & & \vdots \\ P_{n,1} & \cdots & P_{n,n} \end{pmatrix}$$

P is closely related to the adjacency matrix of the coupling graph: every non-zero entry a_{ij} in the adjacency matrix corresponds to a non-zero block P_{ij}. If we have k decoupled subsystems, i.e., if our coupling graph has k independent components, P, thus, is a block-diagonal matrix if a suitable ordering of the fields is used:

$$\underbrace{\begin{pmatrix} \begin{pmatrix} P_{1,1} & \cdots & P_{1,n_1} \\ \vdots & & \vdots \\ P_{n_1,1} & \cdots & P_{n_1,n_1} \end{pmatrix} & & \\ & \ddots & \\ & & \begin{pmatrix} P_{n_{k-1},n_{k-1}} & \cdots & P_{n_{k-1},n_k} \\ \vdots & & \vdots \\ P_{n_k,n_{k-1}} & \cdots & P_{n_k,n_k} \end{pmatrix} \end{pmatrix}}_{P}.$$

This is a quite artificial case as we usually don't choose a multi-field model where we have several completely independent subsystems. In addition, the 'solution' in such a case is straight-forward: We solve the subsystems independent from and possibly parallel to each other. Therefore, we assume in the following that we have a single fully-coupled multi-field problem. However, also in this case, we should have a close look at our permutation matrix P in order to keep the costs for the multi-field coupling as low as possible: if our coupling graph can be partitioned into parts that have only 'outgoing' edges, this means that the respective partition has only a uni-directional coupling to all other fields. In a suitable ordering of the solvers G_i, this case corresponds to an upper block-triangular matrix P:

$$\underbrace{\begin{pmatrix} \begin{pmatrix} P_{1,1} & \cdots & P_{1,n_1} \\ \vdots & & \vdots \\ P_{n_1,1} & \cdots & P_{n_1,n_1} \end{pmatrix} & \cdots & \begin{pmatrix} P_{1,n_{q-1}} & \cdots & P_{1,n_q} \\ \vdots & & \vdots \\ P_{n_1,n_{q-1}} & \cdots & P_{n_1,n_q} \end{pmatrix} \\ & \ddots & \vdots \\ & & \begin{pmatrix} P_{n_{q-1},n_{q-1}} & \cdots & P_{n_{q-1},n_q} \\ \vdots & & \vdots \\ P_{n_q,n_{q-1}} & \cdots & P_{n_q,n_q} \end{pmatrix} \end{pmatrix}}_{P}.$$

In this case, we would use our true multi-field coupling within the q subsystems only: We first solve the system comprising $G_{n_{q-1}}, \ldots, G_{n_q}$, then the subsystem consisting of $G_{n_{q-2}}$, …, $G_{n_{q-1}}$ and so forth until we have solved the last block of coupled fields with $G_1, \ldots, G_{n_1}$.

In special cases, some of these field can be solved in parallel to each other. This is the case if they do not depend on each other but are only indirectly coupled via a third subsystem.

8 Numerical Results II: Fluid with Multiple Structures

8.1 Experiment Settings

We use a second academic example to check the applicability of our method for problems with different characteristics. In this example, we embed several structures in a single fluid domain.

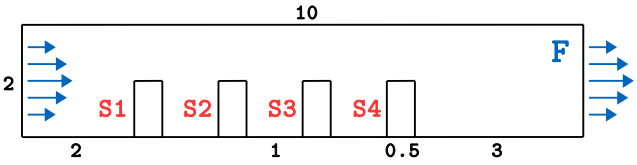

Fig. 9 Scenario sketch: Four structure domains S_1, S_2, S_3, and S_4 are embedded in a flow channel (F). The structure 'towers' are fixed at the bottom of the channel.

Figure 9 depicts the geometry of our second test problem. Four elastic beams S_1, S_2, S_3, S_4 are embedded in a flow channel of size 10×2 m and fixed at the bottom wall of the channel. The structure beams are modeled by St. Venant-Kirchoff cantilevers with Young's modulus $E = 5 \cdot 10^5$ kg/ms^2 and and Poisson-ratio 0.4. The density of the structures is 10 kg/m^3 for S_1, 0.1 kg/m^3 for S_2, 1 kg/m^3 for S_3, and 100 kg/m^3 for S_4 wherwas the fluid density is 1 kg/m^3. Thus, the coupling strength between fluid and structure varies between S_1, S_2, S_3, and S_4.

The fluid is again modeled by means of the incompressible Navier-Stokes equations with the dynamic viscosity $\mu = 1$ kg/ms, the mean velocity of the parabolic inflow profile $U = 50$ m/s. The Reynolds number of the flow is $Re = 100$ (relative to the channel width).

As in the fluid-structure-fluid model problem, we use `Alya` as the physical solver for all domains. All domains are discretized with finite elements, the meshes are matchting at all fluid-structure interfaces. The flow domain is discretized using 4702 elements in an arbitrarily Lagrangian-Eulerian setting, each of the structures has 140 elements in a Lagrangian setting. The timestep size is set to $dt = 10^{-4}$ s. Relative convergence criteria of 10^{-4} are used for all coupling variables. Figure 10 shows the results at $t = 0.02$ s

8.2 Discussion

This subsection presents and discusses the results for the test case described above. For the first 200 time steps using the MIQN(8) coupling scheme with a second order extrapolation for the initial guess, we achieve an average iteration number of 7.71 per time step. We scale all force vectors by a factor of 10^{-6} (compare the discussion in Section 4.2). If we use a concatenation of bi-coupling schemes based on IQn as described in Sect. 4.1.1, we observe divergence already in the first time step.

To get some further insight in the mechanisms of the observed divergence, we additionally simulated the setup with the four structures having a very high density of 10^4 kg/m^3, a scenario that we would expect to be very stable. Table 2 shows the number of iterations required with a concatenation of bi-couplings for each of the involved IQN(8) schemes. We observe good convergence in the first few time steps but a fast increase of iteration numbers starting from time step 5. Thus, even for a scenario whos equivalent with only a single structure is very easy to solve due to the high structure density, the concatenation of bi-coupling IQN schemes does not give the desired results. We can conclude that the instabilty for this case is purely induced by the changing response of partner-solvers in the bi-coupling schemes due to the influence of the other solvers.

	$F-S_1$	$F-S_2$	$F-S_3$	$F-S_4$
step 1	5	5	5	5
step 2	4	4	4	4
step 3	4	4	4	4
step 4	4	4	4	4
step 5	3	11	21	27
step 6	7	7	18	7
step 7	14	14	39	14
step 8	13	34	42	26
step 9	26	50	35	35
step 10	35	35	46	46

Table 2 Iteration counts for the fluid flow with four embedded structures coupled with a concatenation of bi-coupling IQN(8) schemes over the first ten time steps. The fluid in the underlying setup has a density of 1 kg/m^3 whereas all four structures have a very high density of 10^4 kg/m^3.

For the MIQN(8) multi-couling scheme, we achieve the result that we would have expected regarding the high density ratio. Table 3 shows that very few iterations per time step are sufficient.

This examples confirms the conclusion from the results for the fluid-structure-fluid model problem that the MIQN coupling scheme is capable of automatically tackling the physical coupling between multiple fields even in cases where the strength of the coupling varies within the overall system.

	MIQN(8)
step 1	7
step 2	5
step 3	4
step 4	5
step 5	4
step 6	2
step 7	3
step 8	3
step 9	2
step 10	2

Table 3 Iteration counts for the fluid flow with four embedded structures coupled with the MIQN(8) multi-coupling scheme over the first ten time steps. The fluid in the underlying setup has a density of 1 kg/m^3 whereas all four structures have a very high density of 10^4 kg/m^3.

9 Conclusions

In this work, we developed multi-coupling schemes based on either a composition of bi-coupling schemes or a true generalization of the underlying ideas of bi-coupling schemes. We tested those schemes by means of a simple, but still challenging fluid-structure-fluid and fluid with multiple structures model problems.

For the fluid-structure-fluid problem, we observed that, if one fluid-structure interface posseses a weak and the other one a strong interaction, the strong interaction dominates the overall stability and a concatenation of an explicit with an implicit scheme (cf. Section 4.1.1) leads to a stable multi-coupling scheme. If both fluid-structure interfaces show a strong interaction, a concatenation of two implicit coupling schemes does not result in an overall stable scheme, since both interface system hamper each other. For this case, we developed a true multi-coupling scheme, named "multi interface quasi-Newton" (MIQN) scheme by generalizing the ideas that we used in earlier work to deduce parallel FSI coupling schemes ([17,13].

The numerical experiments for the fluid with multiple structures problem confirmed our conclusion that our multi-coupling MIQN schemes are capable of tackling multi-physics problems even in cases with variable physical coupling strength between the involved fields. In addition, we could show that a concatenation of bi-coupling schemes using IQN fails even for scenarios where we would expect the numerical coupling to be stable due to the weak interaction between the fields.

To our knowledge, this is the first time, that a fully implicit black-box multi-coupling scheme is described. This allows to simulate a new range of applications in a partitioned way.

We showed that the multi-coupling idea can be easily generalize to multi-physics problems consisting of arbitrary physical fields. If one group of interface interactions is weak, and the other one strong, it should always be possible to couple all strong interactions with the MIQN scheme and then concatenate MIQN with explicit schemes for each weak interaction.

Acknowledgements: The financial support of the Institute for Advanced Study (IAS) of the Technische Universität München, and of SPPEXA, the German Science Foundation Priority Programme 1648 – Software for Exascale Computing are thankfully acknowledged. `Alya` is developed at the Barcelona Supercomuting Center, by Guillaume Houzeaux, Mariano Vázquez, et al. We want to thank, in particular, Juan Carlos Cajas, who helped to implement the `preCICE` adapter in `Alya`.

References

1. Bazilevs, Y., Takizawa, K., Tezduyar, T.E.: Computational Fluid-Structure Interaction: Methods and Applications. Wiley (2013)
2. Brummelen, E.H.V.: Added Mass Effects of Compressible and Incompressible Flows in Fluid-Structure Interaction. Journal of Applied Mechanics **76** (2009). DOI 10.1115/1.3059565
3. Causin, P., Gerbeau, J.F., Nobile, F.: Added-mass effect in the design of partitioned algorithms for fluid–structure problems. Rapport de recherche, INRIA (2005)
4. Degroote, J., Bathe, K.J., Vierendeels, J.: Performance of a new partitioned procedure versus a monolithic procedure in fluid-structure interaction. Computers & Structures **87** (2009). DOI 10.1016/j.compstruc.2008.11.013
5. Farhat, C., Lesoinne, M.: Two efficient staggered algorithms for the serial and parallel solution of three-dimensional nonlinear transient aeroelastic problems. Computer Methods in Applied Mechanics and Engineering **182** (2000)
6. Gatzhammer, B.: Efficient and flexible partitioned simulation of fluid-structure interactions. Ph.D. thesis, Technische Universität München, Institut für Informatik (2014)
7. Graczyk, M., Moan, T.: A probabilistic assessment of design sloshing pressure time histories in LNG tanks. Ocean Engineering **35** (2008)
8. Haelterman, R., Degroote, J., Heule, D.V., Vierendeels, J.: The quasi-Newton least squares method: A new and fast secant method analyzed for linear systems. SIAM Journal on Numerical Analysis **47** (2009)
9. Houzeaux, G., Vázquez, M., Aubry, R., Cela, J.: A massively parallel fractional step solver for incompressible flows. J. of Comput. Phys. **228** (2009)
10. Küttler, U., Wall, W.A.: Fixed-point fluid–structure interaction solvers with dynamic relaxation. Computational Mechanics **43** (2008). DOI 10.1007/s00466-008-0255-5
11. Lafortune, P., Aris, R., Vázquez, M., Houzeaux, G.: Coupled electromechanical model of the heart: Parallel finite element formulation. Int. J. Num. Meth. Bio. Engng. **28** (2012)

12. Link, G., Kaltenbacher, M., Breuer, M., Döllinger, M.: A 2D finite-element scheme for fluid-solid-acoustic interactions and its application to human phonation. Computer Methods in Applied Mechanics and Engineering **198** (2009). DOI 10.1016/j.cma.2009.06.009
13. Mehl, M., Uekermann, B., Bijl, H., Blom, D., Gatzhammer, B., Zuijlen, A.V.: Parallel Coupling Numercis for Partitioned Fluid-Structure Interaction Simulations. submitted to SIAM SISC (2013)
14. Michler, C.: An interface Newton-Krylov solver for fluid-structure interaction. International Journal for Numerical Methods in Fluids **47** (2004)
15. Minami, S., Yoshimura, S.: Performance evaluation of nonlinear algorithms with line-search for partitioned coupling techniques for fluid-structure interactions. Int. J. Num. Meth. Fluids **64** (2010)
16. Sicklinger, S., Belsky, V., Engelmann, B., Elmqvist, H., Olsson, H., Wüchner, R., Bletzinger, K.U.: Interface Jacobian-based Co-Simulation. Int. J. Num. Meth. Eng. **98** (2014)
17. Uekermann, B., Bungartz, H.J., Gatzhammer, B., Mehl, M.: A parallel, black-box coupling algorithm for fluid-structure interaction. In: Proceedings of ECCOMAS Coupled Problems 2013. Ibiza, Spain (2013)
18. Uekermann, B., Cajas, J.C., Gatzhammer, B., Houzeaux, G., Mehl, M., Vázquez, M.: Towards Partitioned Fluid-Structure Interaction on Massively Parallel Systems. In: Proceedings of WCCM XI/ ECCM V/ ECFD VI. Barcelona, Spain (2014)
19. Vierendeels, J., Lanoye, L., Degroote, J., Verdonck, P.: Implicit coupling of partitioned fluid-structure interaction problems with reduced order models. Computers & Structures **85** (2007). DOI 10.1016/j.compstruc.2006.11.006

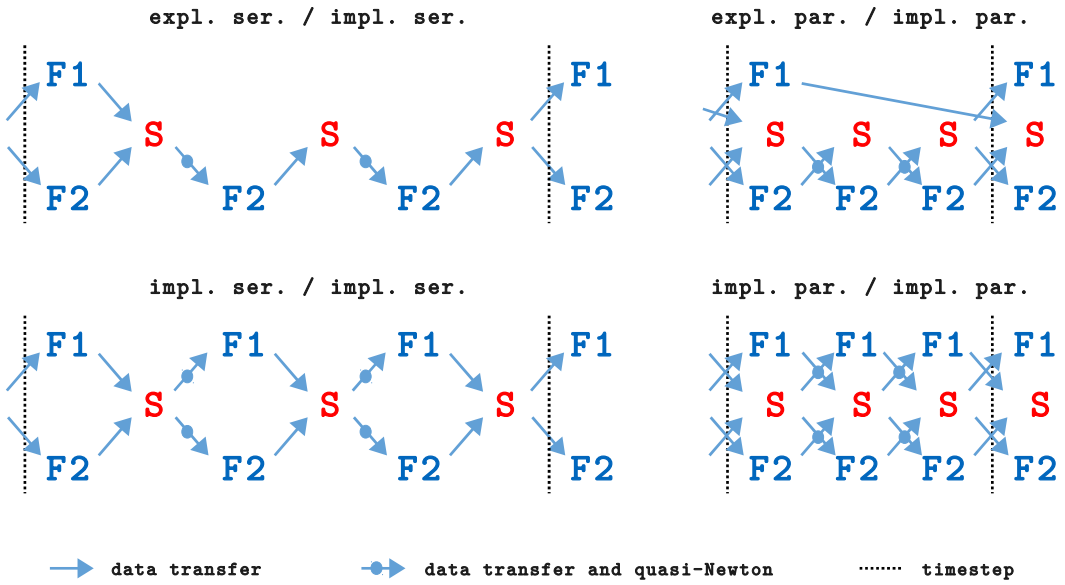

Fig. 4 Execution orders for concatenation of different bi-coupling scheme. Whether the coupling scheme is explicit or implicit, serial or parallel, the execution order differs. The selection of sketches is restricted to reasonable and non-trivial combinations. For sake of simplicity, implicit coupling schemes are assumed to converge in 3 iterations.

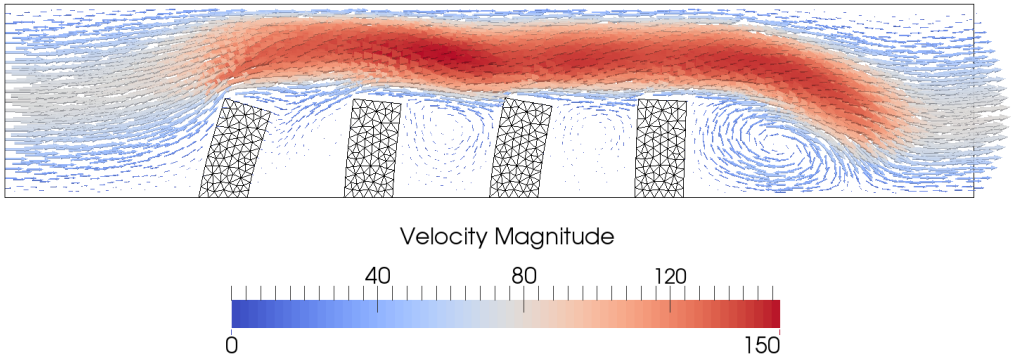

Fig. 10 Velocities and grid deformation for the multiple structure problem at $t = 0.02$. The simulation used the MIQN(8) coupling scheme with a second order extrapolation for the initial guess.